International Journal of Heat and Mass Transfer 176 (2021) 121417

Contents lists available at ScienceDirect

International Journal of Heat and Mass Transfer

journal homepage: www.elsevier.com/locate/hmt

Inverse design of rotating metadevice for adaptive thermal cloaking

Zhan Zhu[a], Xuecheng Ren[a], Wei Sha[b], Mi Xiao[b,c], Run Hu[a,*], Xiaobing Luo[a]

[a] School of Energy and Power Engineering, Huazhong University of Science and Technology, Wuhan 430074, China
[b] State Key Laboratory of Digital Manufacturing Equipment and Technology, Huazhong University of Science and Technology, Wuhan, 430074, China
[c] No. 55 Research Institute of China North Industries Group Corporation, Changchun, 130012, China

ARTICLE INFO

Article history:
Received 5 February 2021
Revised 23 April 2021
Accepted 24 April 2021
Available online 24 May 2021

Keywords:
Thermal metamaterials
Thermal cloaking
Rotating metadevice
Effective thermal conductivity

ABSTRACT

Thermal metamaterials have been extensively studied due to their extraordinary properties beyond natural materials and offered great flexibilities to tune heat flow for desired thermal functionalities, like thermal cloaking, concentrating, rotating, etc. Whereas, the thermal properties of thermal metamaterials are usually fixed once the configuration and the constituent materials are designed and fabricated. For instance, the thermal cloaking effect may be deteriorated when background changes, which limits its practical application significantly. By deducing the effective thermal conductivities of rotating objects, we propose an adaptive thermal cloaking metadevice that is composed by three rotating layers with different roles. The joint effect of three rotating layers makes the effective thermal conductivity a real number on the reciprocity line for feasible implementation. When background changes, we only need change the angular velocities rather than change the configuration or the constituent materials to restore the cloaking effect, which is much more convenient and real-time for practical applications. The underlying physics of the rotating thermal cloak is discussed to identify the key parameters and upper and lower limits of the effective thermal conductivity for further improving the cloaking effect. The present study can trigger more rotating metadevices for novel applications beyond thermal cloaking.

1. Introduction

Thermal metamaterials have been attracting great interest since they have exhibited extraordinary properties beyond natural materials and offered great advantages for tuning heat flow almost at will. Based on thermal metamaterials, numerous thermal metadevices have been proposed for diverse functionalities, such as thermal cloak, thermal concentrator, thermal rotator, thermal camouflage, thermal illusion, etc. [1-25]. However, once the configuration and the constituent materials of the thermal metadevices are designed, the corresponding functionality can only be achieved at certain conditions [26-33]. In other words, most thermal metamaterials are usually unable to dynamically adapt to the change of environment. Even by changing the configuration or the constituent materials, the effective material parameters can only be switched between a finite number of discrete values, disabling the continuous regulation of the effective materials and the flexibility of these thermal metadevices. Let us take thermal cloak for an example. The methods of designing thermal cloak are mainly based on transformation thermotics [1-3] and scattering cancellation techniques [4]. Both methods require the thermal conductivity tensor of the cloak meets certain conditions to achieve thermal cloaking effect. In transformation thermotics, $\kappa' = diag(\frac{r-a}{r}, \frac{r}{r-a})\kappa_b$, where a is the inner radius of the annular cloak in cylindrical coordinate, and κ_b is the thermal conductivity of the background; while in scattering cancellation, for a two-dimensional bilayer thermal cloak [4], $\kappa_2'=0$,$\kappa_3' = ((2c^3+b^3)/2(c^3-b^3))\kappa_b$, where b and c are the radii of the outer layer. It is seen that the thermal conductivity of the cloak κ' is related to the thermal conductivity of the background κ_b, which means that the thermal cloaking effect cannot be maintained when the background changes. To restore the cloaking effect in the changing background, the material configuration or the constituent materials must be changed accordingly.

Recently, thermal convection [34-40] has garnered increasing attention as it can be used to continuously control the effective thermal conductivity by introducing velocity as another degree of freedom. But convection will break the Onsager reciprocity that exists in macroscopic heat conduction [34,35,41] and resulting asymmetric effective thermal conductivity tensor will distort the temperature field around the rotating object to some extent. Li et al. proposed that the effective thermal conductivity of the rotating object is usually a complex number due to the break of the reciprocity [35]. To restore the reciprocity and achieve the desired solid-like effect, they make the effective complex thermal conduc-

* Corresponding author.
E-mail address: hurun@hust.edu.cn (R. Hu).

https://doi.org/10.1016/j.ijheatmasstransfer.2021.121417
0017-9310/

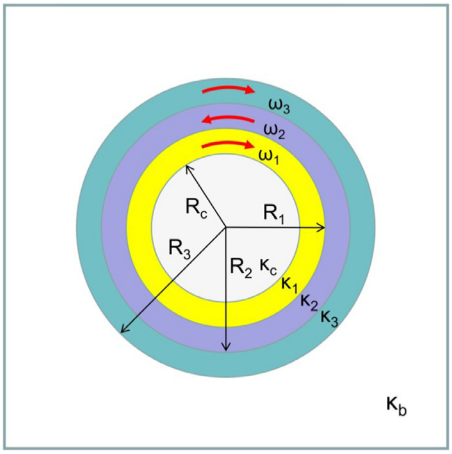

Fig. 1. Schematic diagram of the adaptive cloak.

tivity as a pure real number by reasonably adjusting the angular velocities [34].

In this work, we design a multi-layer adaptive thermal cloak that can adapt to the change of background and maintain the cloaking effect simultaneously. We firstly deduced the formula of the effective thermal conductivity of the three layers as we found that adaptive thermal cloaking can be achieved by three rotating layers. The inner rotating layer is used to maintain the cloaking region isothermal. The remaining two layers are designed to make the effective thermal conductivity as a real number which equals to the thermal conductivity of the background so that isotherms are parallel for ideal thermal cloaking effect. Finite element simulations were conducted to validate the formula and the adaptive thermal cloaking effect, and related discussions were presented to explain the underlying mechanisms. The present study is expected to trigger more rotating metadevices for novel applications beyond thermal cloaking.

2. Theoretical analysis

Considering a two-dimensional cylindrical system, a temperature gradient is launched by maintaining two sides of a square background ($L \times L$) with thermal conductivity κ_b at constant temperatures T_R and T_L. The upper and lower boundaries are thermally insulated. The cylindrical cloak, which consists of three concentric annuluses, as shown in Fig. 1, is used to cloak the center object. The thermal conductivities and radii are illustrated in Fig. 1. Diffusivities of three ring layers are D_1, D_2 and D_3, respectively. The circular region is static while the angular velocities of three ring layers are ω_1, ω_2 and ω_3, respectively. The first layer rotates clockwise, the second layer rotates counterclockwise and the third layer rotates clockwise. The governing equations for the temperature fields T_c in $r \le R_c$, T_1 in $R_c \le r \le R_1$, T_2 in $R_1 \le r \le R_2$, T_3 in $R_2 \le r \le R_3$, T_b in $r \ge R_3$ are

$$
\begin{aligned}
&\frac{\partial^2 T_{b,c}}{\partial r^2} + \frac{1}{r}\frac{\partial T_{b,c}}{\partial r} + \frac{1}{r^2}\frac{\partial^2 T_{b,c}}{\partial \theta^2} = 0 \; r \le R_c, r \ge R_3 \\
&\frac{\partial^2 T_{1,2,3}}{\partial r^2} + \frac{1}{r}\frac{\partial T_{1,2,3}}{\partial r} + \frac{1}{r^2}\frac{\partial^2 T_{1,2,3}}{\partial \theta^2} = \frac{\omega_{1,2,3}}{D_{1,2,3}}\frac{\partial T_{1,2,3}}{\partial \theta} R_c \le r \le R_3
\end{aligned}
\tag{1}
$$

By variable separation method, the temperature profile could be explicitly written as $T(r,\theta) = F(r)\cdot G(\theta)$ where $G(\theta)$ is a periodic function, and Eq. (1) can be solved analytically. Note that the temperature usually varies slowly, the $G(\theta)$ can be given as the function of θ as $G(\theta) = e^{i\theta}$. The temperature field needs to meet the following equation:

$$
T(r,\theta) = T_0 + \frac{1}{2}\left[F(r)\cdot e^{i\theta} + \overline{F(r)}\cdot e^{-i\theta}\right] \tag{2}
$$

where the overline denotes conjugation in complex number and T_0 is a constant. Substituting Eq. (2) into Eq. (1), the general solutions of $F(r)$ can be described as:

$$
\begin{aligned}
&F_b(r) = Ar + z_b r^{-1}, r \ge R_3 \\
&F_3(r) = z_5 M(\omega_3, r) + z_6 N(\omega_3, r), R_2 \le r \le R_3 \\
&F_2(r) = z_3 M(\omega_2, r) + z_4 N(\omega_2, r), R_1 \le r \le R_2 \\
&F_1(r) = z_1 M(\omega_1, r) + z_2 N(\omega_1, r), R_c \le r \le R_1 \\
&F_c(r) = z_c r, r \le R_c
\end{aligned}
\tag{3}
$$

where the coefficients $z_c, z_b, z_1 - z_6$ are determined by the matching conditions of temperature and heat fluxes. $M(\omega,r)$ and $N(\omega,r)$ are:

$$
M(\omega,r) = \begin{cases} I_1\left(\sqrt{i\omega/D}r\right) & \omega \neq 0 \\ r & \omega = 0 \end{cases},
$$

$$
N(\omega,r) = \begin{cases} K_1\left(\sqrt{i\omega/D}r\right) & \omega \neq 0 \\ 1/r & \omega = 0 \end{cases} \tag{4}
$$

where $I_1(x)$ and $K_1(x)$ are the first-order modified Bessel functions of the first and second kind. D is the diffusivity of the region rotating at ω. Combining Eqs. (1-4), we can obtain the effective thermal conductivity of the multilayer rotating object:

$$
\kappa^*_{c\sim n} = \kappa_n \frac{\kappa_n s_n - \kappa^*_{c\sim(n-1)} r_n}{\kappa_n q_n - \kappa^*_{c\sim(n-1)} p_n} \tag{5}
$$

Therefore, the effective thermal conductivity of this three-layer object can be deduced by iterating Eq. (5). For $n = 1$, $\kappa^*_{c\sim1} = \kappa_s \frac{\kappa_s s_1 - \kappa^*_{c\sim0} r_1}{\kappa_s q_1 - \kappa^*_{c\sim0} p_1}$, where $\kappa^*_{c\sim0}$ is κ_c. For $n = 2$, $\kappa^*_{c\sim2} = \kappa_s \frac{\kappa_s s_2 - \kappa^*_{c\sim1} r_2}{\kappa_s q_2 - \kappa^*_{c\sim1} p_2}$, where $\kappa^*_{c\sim1}$ has already been deduced by using Eq. (5). Similarly, $\kappa^*_{c\sim3}$ can be obtained as

$$
\kappa^*_{c\sim3} = \kappa_s \frac{\kappa_s(q_1q_2s_3 - s_1p_2s_3 - q_1s_2r_3 + s_1r_2r_3) + \kappa_c(r_1p_2s_3 - p_1q_2s_3 + p_1s_2r_3 - r_1r_2r_3)}{\kappa_s(q_1q_2q_3 - s_1p_2q_3 - q_1s_2p_3 + s_1r_2p_3) + \kappa_c(r_1p_2q_3 - p_1q_2q_3 + p_1s_2r_3 - r_1r_2p_3)} \tag{6}
$$

where κ_s is the thermal conductivity of three ring layers. Here we set the thermal conductivity and the diffusivity of three ring layers as the same, i.e. $\kappa_s{=}\kappa_1{=}\kappa_2{=}\kappa_3$, $D_1{=}D_2{=}D_3$. The four cross-products p_n, q_n, r_n, s_n can be determined as

$$
\begin{bmatrix} p_n \\ q_n \\ r_n \\ s_n \end{bmatrix}^T = \begin{bmatrix}
\det\begin{bmatrix} M(\omega_n,R_n) & N(\omega_n,R_n) \\ M(\omega_n,R_{n-1}) & N(\omega_n,R_{n-1}) \end{bmatrix} \\
\det\begin{bmatrix} M(\omega_n,R_n) & N(\omega_n,R_n) \\ M'(\omega_n,R_{n-1}) & N'(\omega_n,R_{n-1}) \end{bmatrix} \\
\det\begin{bmatrix} M'(\omega_n,R_n) & N'(\omega_n,R_n) \\ M(\omega_n,R_{n-1}) & N(\omega_n,R_{n-1}) \end{bmatrix} \\
\det\begin{bmatrix} M'(\omega_n,R_n) & N'(\omega_n,R_n) \\ M'(\omega_n,R_{n-1}) & N'(\omega_n,R_{n-1}) \end{bmatrix}
\end{bmatrix}^T
\begin{bmatrix} 1 & 0 & 0 & 0 \\ 0 & R_{n-1} & 0 & 0 \\ 0 & 0 & R_n & 0 \\ 0 & 0 & 0 & R_{n-1}R_n \end{bmatrix} \tag{7}
$$

Here, R_0 is R_c. It should be noted that $M'(\omega,r)$ and $N'(\omega,r)$ here only take derivatives of $M(\omega,r)$ and $N(\omega,r)$ to r. The effective thermal conductivity in Eq. (6) is independent of the external parameters (L,κ_b,T_R,T_L) and only influenced by the structure parameters.

Based on convection, rotating allows continuous adjustment of the effective thermal conductivity over a wide range breaking the limit of Maxwell-Garnett mixing rule. However, $\kappa^*_{c\sim3}$ ($\kappa^*_{c\sim3}$ is mentioned as κ^* hereinafter for simplification) is a complex number because of the properties of the modified Bessel functions. The imaginary part of the effective thermal conductivity essentially comes from the broken reciprocity, resulting in that the temperature field around rotating objects will be distorted to some extent. Therefore, it is not generally applicable to the regulation requirements of conventional thermal metamaterials [28,39,42,43]. To eliminate the advection effect of the rotating layers, the angular velocity of each layer should be set reasonably to make the calculated effective thermal conductivity as a pure real number. The real-number effective thermal conductivity restores the reciprocity and makes rotating objects achieve a solid-like effect. Obviously, the direction of rotating should be opposite to cancel each other out so that the effective thermal conductivity can be a real number. With reasonable adjustment of the angular velocities, the effective thermal conductivity can be continuously changed to adapt the change in the environment while maintaining the thermal cloaking effect.

3. Results and discussions

Based on the effective thermal conductivity obtained above, we design an adaptive cloak as shown in Fig. 1. The whole simulation region is 200×200 mm^2. Here we set κ_c=κ_s=κ_1=κ_2=κ_3=50 W m^{-1} K^{-1}, D_1=D_2=D_3=13.3 mm^2 s^{-1}, R_c=0.03 m, R_1=0.04 m, R_2=0.05 m, R_3=0.06 m. Ideal thermal cloaking effect requires (1) The temperature gradient vanishes in the center region where the object is placed and (2) The isotherms outside the cloak region are parallel. To achieve these requirements, a three-ring-layer structure is set up specifically. The first layer has a large angular velocity to eliminate the temperature gradient inside the center region. The angular velocities of the second and the third layers should be adjusted properly to make the effective thermal conductivity κ^* as a real number and equal to the thermal conductivity of the background κ_b so as to make the external isotherms parallel according to the scattering cancellation principle.

Fig. 2a illustrates the simulated temperature fields with varying angular velocities ω_1. It is seen in Fig. 2a that when ω_1 is small (I, 0.2 rad s^{-1}), the temperature inside the circular region is not uniform, while ω_1 is large enough (III, 1.3 rad s^{-1}), the temperature gradient inside the circular region vanishes. Meanwhile, the isotherms outside the cloak are always vertical and uniform. Fig. 2b shows the simulated temperature fields with fixed angular velocities (ω_1: 1.3 rad s^{-1}, ω_2: −0.5 rad s^{-1}, ω_3: 0.05688 rad s^{-1}) and varying background's thermal conductivities from 100, 166, to 200 W m^{-1}K^{-1}. From Eq. (6), the effective thermal conductivity κ^* in this case is calculated as 166 W m^{-1} K^{-1}. When κ^* is larger (I) or smaller (III) than κ_b, the external isotherms are not parallel and the thermal cloaking effect is deteriorated. Only when κ^* equals κ_b, the external isotherms are parallel, which meets the second criterion of thermal cloaking. Fig. 2c shows how the effective thermal conductivity of the circular region and first layer varies with different ω_1. When ω_1 increases, the real part and the imaginary part of the effective thermal conductivity increase accordingly, which is why the first criterion of thermal cloaking effect can be achieved at large ω_1. To quantify the thermal cloaking effect, temperature profiles along the horizontal cutline at y=0 (red lines) and vertical cutline at x=8 cm (black lines) are shown in Fig. 2d. The temperature gradient in the circular region decreases with the increasing of ω_1 and when ω_1 is 1.3 rad s^{-1}, the temperature gradient is almost zero, which validates the first criterion of thermal cloaking effect. When κ^* equals κ_b, the temperature profile is uniform as well, validating the parallel isotherms of the thermal cloaking effect.

To sum up, the three-layer structure can be adjusted to achieve different effective thermal conductivities and thermal cloaking effect can be accomplished when: (1) ω_1 is large enough to make the temperature gradient vanish inside the cloaking region; (2) ω_2 and ω_3 are properly designed to make κ^* as a real number that equals to κ_b. For the two-layer rotating structure, the angular velocities of these two layers should be regulated properly to make the effective thermal conductivity the same as background's thermal conductivity. When the background changes, the cloaking effect will not be maintained if the angular velocity of the first layer is small in a certain case. While, for the three-layer scheme, the adaptability of the changing background has more freedom because three angular velocities can be adjusted. If more layers are used for adaptive cloak, like four layers, the adaptive cloaking effect can be achieved at the expense of more complicated structure and implementation.

So far, we have only demonstrated the static cloaking effect, which cannot be called as 'adaptive'. For this end, the angular velocities need to be calculated at different κ_b to meet those two criteria of thermal cloak. From Eq. (6), the effective thermal conductivity can be calculated by inputting the radius, diffusivity and angular velocity. In return, the angular velocities can also be inversely calculated by providing the radius, diffusivity and expected thermal conductivity. When background changes, the proper angular velocities can be calculated inversely to maintain the cloaking effect.

When the background (κ_b) changes, we can calculate angular velocities inversely by Eq. (6), and then modify the angular velocities manually or automatically to maintain the cloaking effect. To make κ^* equal to κ_b, κ^* should be a real number firstly to keep the reciprocity. For a certain ω_1, the matching ω_2 and ω_3 are not unique, and so is the real-number effective thermal conductivity. As shown in Fig. 3a, the matching ω_2 and ω_3 can be plotted as ω_1-dependent lines to make the effective thermal conductivity as a real number. Such lines are called as reciprocal lines. For a certain ω_1, the matching ω_3 increases rapidly at first and then decreases gradually as ω_2 increases. For the same ω_2, the larger ω_1 is, the smaller matching ω_3 is. The reason is that both of the first layer and the third layer rotate clockwise but the second layer rotates counterclockwise. If ω_1 is larger, the matching ω_3 can be smaller accordingly. It is seen that ω_1 matters for the matching ω_3 only at the beginning. This is because when ω_2 increases gradually, its influence on κ^* is much greater than that of ω_1. We can also find that ω_2 and ω_3 differ by 1–2 orders of magnitude, which proves the outermost layer has the greatest influence on κ^*. When ω_2 changes in a large range, ω_3 only changes in a small range and the matching conditions can be achieved. After calculating the reciprocal line, the real-number κ^* can be calculated by using three angular velocities on the reciprocal line. As shown in Fig. 3b, with the increasing of ω_2, κ^* decreases at the beginning and then converges gradually. The reason for the initial decrease of κ^* is that the first layer and the second layer rotate reversely, and when ω_2 increases gradually from zero, the effect of clockwise rotation of the first layer will be compromised at the beginning. After completely canceling the influence of the first layer, the counterclockwise rotation of the second layer matters dominantly, so κ^* increases when ω_2 increases. κ^* converges eventually, which means there is an upper limit of κ^*. For different ω_1, the influence is also only at the initial stage where ω_1 plays a major role. The smaller ω_1 is, the smaller κ^* is. According to Fig. 3b, the tunable range of κ^* is limited. Here, the regulatory range of κ^* is about 100–250 W m^{-1} K^{-1}, which surprisingly validates that rotating makes metamaterials beyond the Maxwell-Garnett formula (All thermal conductivities here are 50 W m^{-1} K^{-1}). That is to say, the range of κ_b that the thermal cloak can

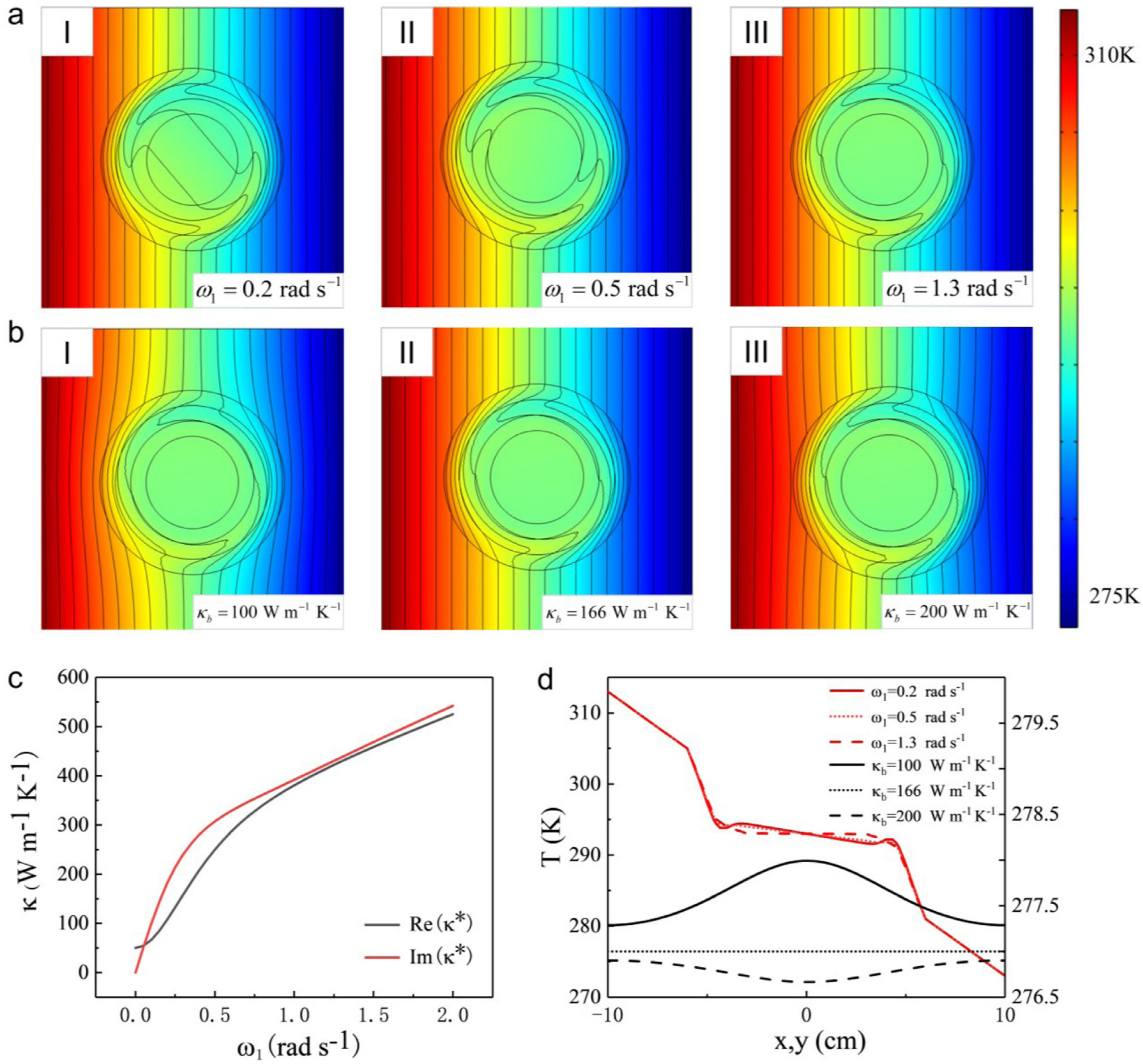

Fig. 2. Simulation validations of thermal cloaking effect with varying parameters. (a) Simulated temperature fields with varying ω_1 from 0.2, 0.5, to 1.3 rad s^{-1}, respectively. (b) Simulated temperature fields with varying thermal conductivities of background from 100, 166, to 200 W m^{-1} K^{-1} and fixed angular velocities (ω_1:1.3 rad s^{-1}, ω_2:−0.5 rad s^{-1} and ω_3:0.05688 rad s^{-1}). (c) The ω_1-dependent real part and imaginary part of the effective thermal conductivity of circular region and the first layer. (d) Temperature profiles along cutlines of y=0 (red lines) and x=8 cm (black lines). (For interpretation of the references to colour in this figure legend, the reader is referred to the web version of this article.)

adapt to is within 100–250 W m^{-1} K^{-1}. Three κ_b (120 W m^{-1} K^{-1}, 186 W m^{-1} K^{-1} and 230 W m^{-1} K^{-1}, respectively) are selected to test the adaptive thermal cloaking effect. As shown in Fig. 3c, the thermal cloaking effects are all achieved ideally by changing ω_2 and ω_3. These setting parameters of the three selected cloaks are marked in Figs. 3a and 3b. If κ_b changes within the tunable range of κ^*, we can find appropriate ω_2 and ω_3 to achieve good thermal cloaking effect even when κ_b changes continuously, which is almost impossible for traditional thermal cloak.

Next, to explore the physical significance of the three angular velocities, the influence of angular velocities on κ^* is further analyzed in Fig. 4. We discuss the real part and the imaginary part respectively. The real part and the imaginary part of κ^* are related to dissipation and propagation. In Fig. 4a, when ω_2 are −0.1 rad s^{-1} and −0.3 rad s^{-1}, Re(κ^*) decreases at first and then increases and finally converges to a certain value. The reason why it decreases at first is the offset effect by different rotating directions of the first and second layer. When ω_2 is 0.7 rad s^{-1}, Re(κ^*) increases at first and then decreases slowly. While Im(κ^*) varies differently at different ω_2. ω_1 has little influence on κ^*, where the regulatory range is about a few dozen. Similarly, Re(κ^*) and Im(κ^*) both decrease and then increase because of the offset effect when ω_2 increases. The regulatory range for different ω_2 is a few hundred, which is larger than that for ω_1. For different ω_3, Re(κ^*) decreases and then increases due to the offset effect while Im(κ^*) keeps increasing. Rotating of the third layer has the strongest influence on the effective thermal conductivity. Different from the first two layers, κ^* does not converge to a certain value when ω_3 increases, and thus the influence of the outer layer is more significant on the effective thermal conductivity.

To make the thermal cloak have a wider range of regulation, we also explore the upper and lower limits of κ^*. Obviously, κ^* is

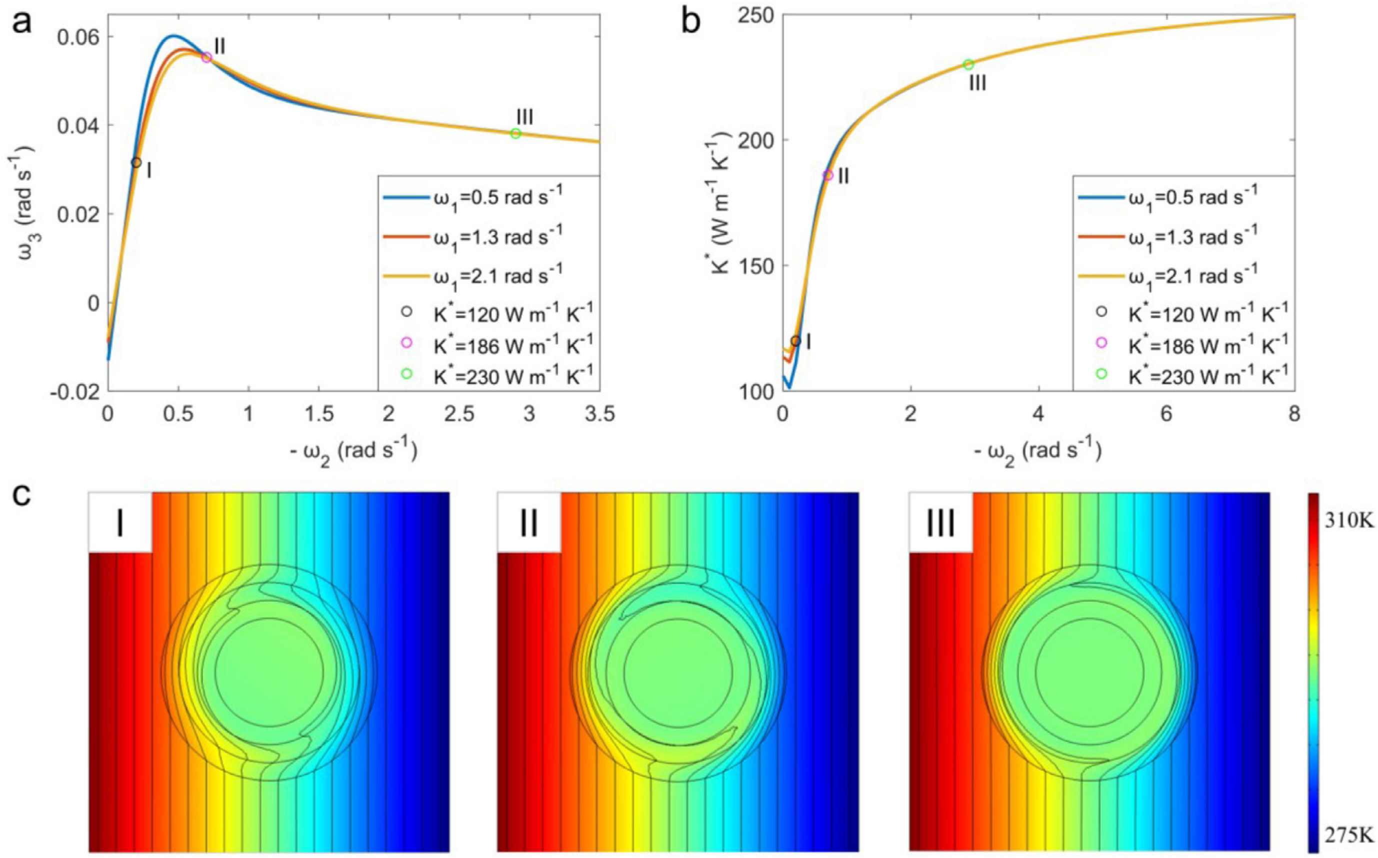

Fig. 3. Discussion on the reciprocal line of κ^* for the adaptive thermal cloak. (a) Reciprocal line for different ω_1. (b) The real-number effective thermal conductivity on three reciprocal lines. (c) Simulations of the adaptive thermal cloak. κ_b for I-III are 120 W m^{-1} K^{-1}, 186 W m^{-1} K^{-1}, 230 W m^{-1} K^{-1}, respectively. Angular velocities are calculated respectively. ω_1,ω_2,ω_3 are 1.3 rad s^{-1}, −0.2 rad s^{-1}, 0.031588 rad s^{-1} for I. 1.3 rad s^{-1}, −0.7 rad s^{-1}, 0.055290 rad s^{-1} for II. 1.3 rad s^{-1}, −2.9 rad s^{-1}, 0.038097 rad s^{-1} for III.

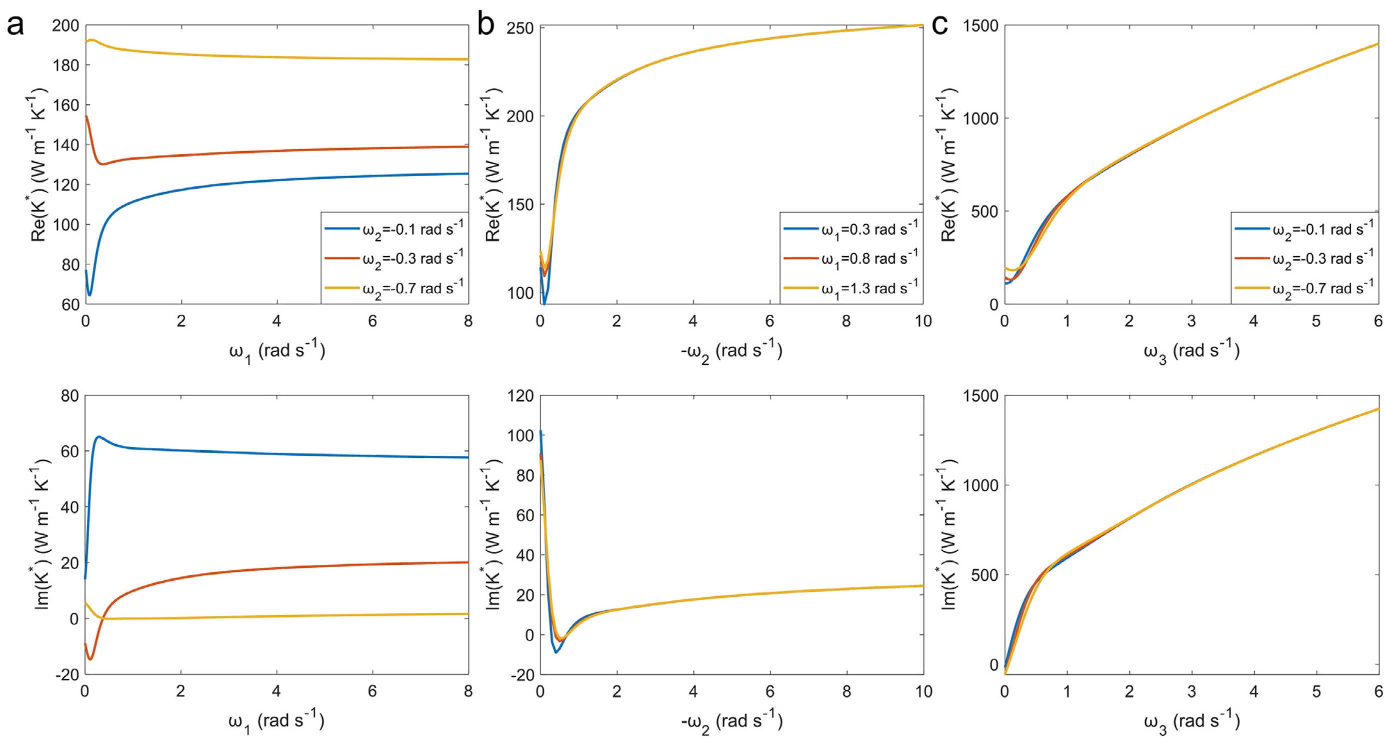

Fig. 4. The influence of three angular velocities on the real part and the imaginary part of κ^*. (a) The influence of ω_1 on κ^* at different ω_2 with fixed ω_3(0.055290 rad s^{-1}). (b) The influence of ω_2 on κ^* at different ω_1 with fixed ω_3(0.055290 rad s^{-1}). (c) The influence of ω_3 on κ^* at different ω_2 with fixed ω_1(1.3 rad s^{-1}).

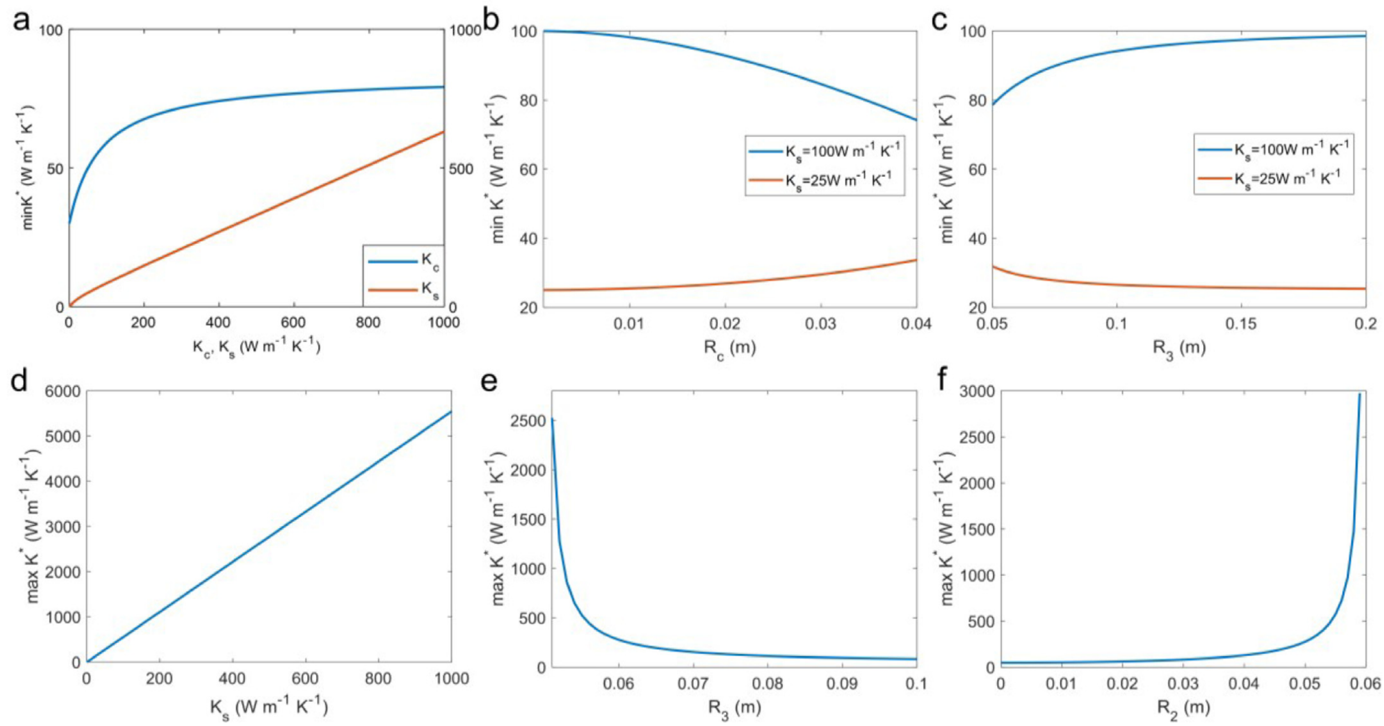

Fig. 5. The influence of each parameter on min κ^* and maxκ^*. (a-c) The influence of each parameter on min κ^*. (d-f) The influence of each parameter on maxκ^*. For subfigures (a-f), κ_c=κ_s=50 W m^{-1} K^{-1},R_c=0.03 m,R_1=0.04 m,R_2=0.05 m,R_3=0.06 m.

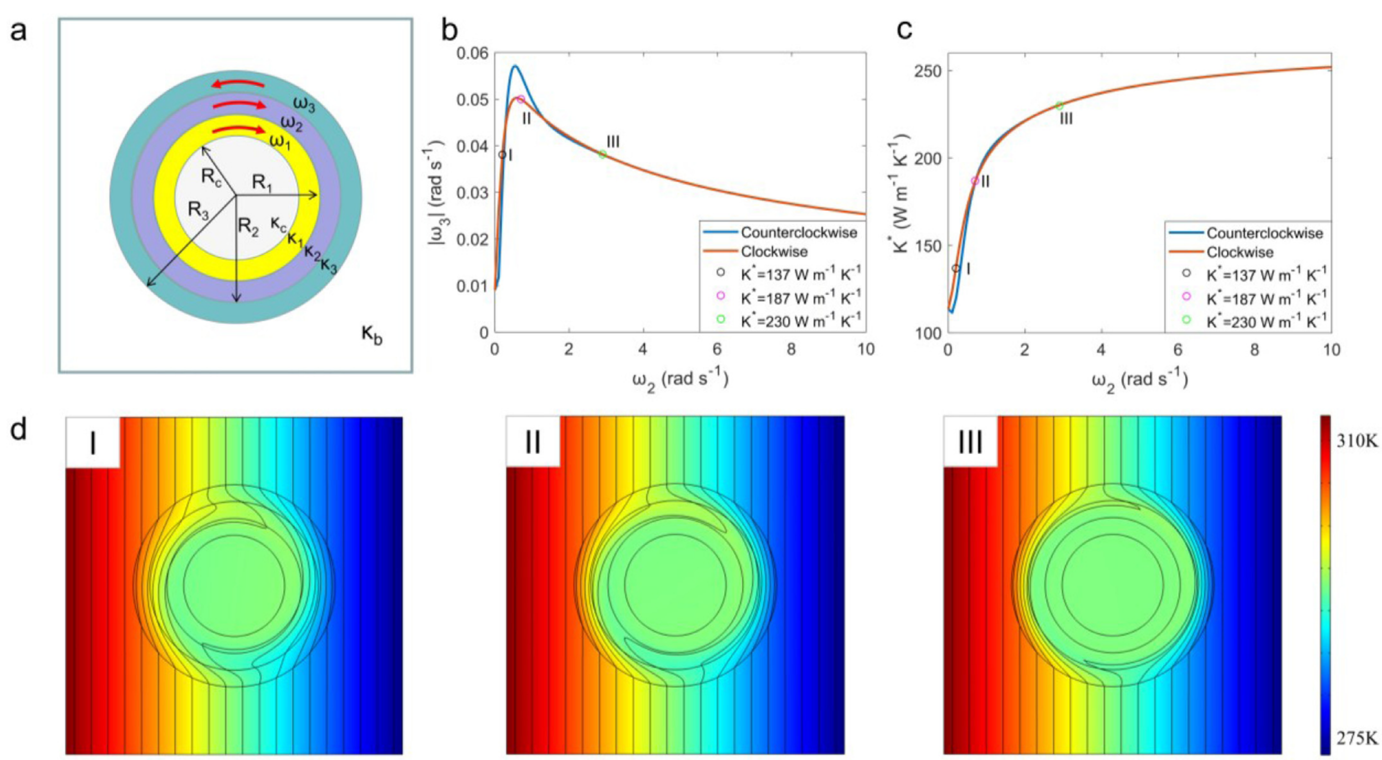

Fig. 6. The influence of reverse rotation in the second and the third layers. (a) Schematic diagram of reverse rotation in the second and the third layers. (b) Comparison of reciprocal lines when the second layer rotates counterclockwise (the third layer rotates clockwise) and clockwise (the third layer rotates counterclockwise). (c) Comparison of κ^* on the reciprocal lines. (d) Simulations of the adaptive cloak when κ_b changes. κ_b for I-III are 137 W m^{-1} K^{-1}, 187 W m^{-1} K^{-1}, 230 W m^{-1} K^{-1}. For I, ω_1: 1.3 rad s^{-1}, ω_2: 0.2 rad s^{-1}, ω_3: −0.038103 rad s^{-1}. For II, ω_1: 1.3 rad s^{-1}, ω_2: 0.7 rad s^{-1}, ω_3: −0.049999 rad s^{-1}. For III, ω_1: 1.3 rad s^{-1}, ω_2: 2.9 rad s^{-1}, ω_3: −0.038182 rad s^{-1}.

the smallest when three angular velocities are all zero. By using the properties of $M(\omega, r)$ and $N(\omega, r)$, the lower limit of κ^* can be derived as

$$\min\kappa^* = \kappa_s \cdot \frac{\left(\frac{\kappa_c}{\kappa_s} - 1\right)\left(1 + \frac{{R_c}^2}{{R_3}^2}\right) + 2}{\left(\frac{\kappa_c}{\kappa_s} - 1\right)\left(1 - \frac{{R_c}^2}{{R_3}^2}\right) + 2}. \tag{8}$$

It is seen from Eq. (8) that the minimum value of κ^* is only related to parameters of the structure (κ_c,κ_s,R_c,R_3). Fig. 5a-c illustrate the influence of each parameter on $\min\kappa^*$. $\min\kappa^*$ increases with the increasing of κ_c and κ_s. The influence of R_c and R_3 depends on the sign of $(\kappa_c/\kappa_s - 1)$. The upper limit of κ^* is taken when $\omega_2 = \infty$. The modified Bessel functions have the following properties: $\lim\limits_{x\to\infty} I'_1(x) = \lim\limits_{x\to\infty} I_1(x)$, $\lim\limits_{x\to\infty} K'_1(x) = \lim\limits_{x\to\infty} K_1(x)$. When $\omega_2 = \infty$, the matching ω_3 on the reciprocal line is zero. Therefore, the formula of $\max\kappa^*$can be obtained as

$$\max\kappa^* = \kappa_s \cdot \frac{R_3^2 + R_2^2}{R_3^2 - R_2^2}. \tag{9}$$

Similarly, $\max\kappa^*$ is only related to parameters of the structure (κ_s,R_2,R_3). Fig. 5d-f illustrate the influence of each parameter on $\max\kappa^*$. When R_3 is much larger than R_2, $\max\kappa^*$ approaches κ_s, which is reasonable in practice. When R_2 approaches R_3, $\max\kappa^*$ can be infinite. Parameters can be chosen properly to get a satisfying range of κ^* by using Eqs. (8) and (9), which provide a basis for choosing parameters of the adaptive thermal cloak. For example, to obtain a wide range of regulation, best parameters can be calculated within the range of $\max\kappa^*$ and $\min\kappa^*$. What's more, to get a higher (lower) $\max\kappa^*$ ($\min\kappa^*$), the required parameters in Eq. (8) or Eq. (9) can be adjusted accordingly. The upper and lower limits of more multilayered structures can be derived as well in a similar way.

Finally, we explore how the reciprocal line and κ^* on the reciprocal line change when the second and the third layers rotate reversely, as shown in Fig. 6a. Can the matching ω_3 for a certain ω_2 be smaller by changing the directions of ω_2 and ω_3 so that we can reduce the input of power? Or can we get a wider regulation range of κ^* for certain angular velocities by changing the directions of ω_2 and ω_3? From Fig. 6b, there is a difference of ω_3 at around ω_2=1 rad s^{-1} when the second and the third layers rotate reversely, which can reduce input of power to some extent. Fig. 6c shows that the influence of rotating reversely on κ^* is concentrated in small-ω_2 region. The same effective thermal conductivity can be obtained from a smaller angular velocity after rotating reversely. Fig. 6d is the simulation of the adaptive reverse-cloak at different κ_b. In different background, the cloaking effect is still achieved well only by changing angular velocities. Parameters of three simulations are marked in Fig. 6b and c. Finally, some discussions about experimental validations are provided. The three layers can rotate with motors and gears on their bottom surfaces, referring to implementation of the two-layer structure [34]. Thermal conductive silicone grease can be used to fill the gaps between the object, the layers and background, which helps to eliminate the interface thermal resistance in the experiment.

4. Conclusion

In this paper, we derive the effective thermal conductivity of the three-layer rotating metadevice and design a three-rotating-layer adaptive thermal cloak inversely. The inner rotating layer is used to maintain the cloaking region isothermal. The remaining two layers are designed to make the effective thermal conductivity as a real number which equals to the thermal conductivity of the background so that isotherms are parallel for adaptive thermal cloaking. When background changes, we only need change the angular velocities rather than change the configuration or the constituent materials to restore the cloaking effect, which is much more convenient and real-time for practical applications. Both finite element simulations and subsequent analysis are carried out to explore the influence of each angular velocity on the effective thermal conductivity, the upper and lower limits of the effective thermal conductivity, and the influence of reverse rotation. Beyond thermal cloaking, more thermal functionalities and novel applications are expected to achieve by resorting to the rotating metadevices in the near future.

Declaration of Competing Interest

There are no conflicts of interest.

CRediT authorship contribution statement

Zhan Zhu: Investigation, Methodology, Writing - original draft. **Xuecheng Ren:** Investigation, Data curation. **Wei Sha:** Writing - review & editing. **Mi Xiao:** Writing - review & editing. **Run Hu:** Conceptualization, Supervision, Writing - review & editing. **Xiaobing Luo:** Writing - review & editing.

Acknowledgments

We acknowledge financial support from the Natural National Science Foundation of China (No. 52076087), Wuhan City Science and Technology Program (No. 2020010601012197), Wuhan City Natural Science Foundation of Hubei Province (No. 2019CFA059), and the Open Project Program of No. 55 Research Institute of China North Industries Group Corporation.

References

[1] C.Z. Fan, Y. Gao, J.P. Huang, Shaped graded materials with an apparent negative thermal conductivity, Appl. Phys. Lett 92 (2008) 251907.
[2] T. Chen, C.-N. Weng, J.-S. Chen, Cloak for curvilinearly anisotropic media in conduction, Appl. Phys. Lett. 93 (2008) 114103.
[3] S. Guenneau, C. Amra, D.J.O.E. Veynante, Transformation thermodynamics: cloaking and concentrating heat flux, Opt. Express 20 (2012) 8207.
[4] T. Han, X. Bai, D. Gao, J.T. Thong, B. Li, C.W. Qiu, Experimental demonstration of a bilayer thermal cloak, Phys. Rev. Lett. 112 (2014) 054302.
[5] R. Hu, S. Huang, M. Wang, X. Luo, J. Shiomi, C.W. Qiu, Encrypted thermal printing with regionalization transformation, Adv. Mater. 31 (2019) 1807849.
[6] J.Y. Li, Y. Gao, J.P. Huang, A bifunctional cloak using transformation media, J. Appl. Phys 108 (2010) 074504.
[7] R. Hu, S. Huang, M. Wang, L. Zhou, X. Peng, X. Luo, Binary thermal encoding by energy shielding and harvesting units, Phys. Rev. Appl. 10 (2018) 054032.
[8] R. Hu, S. Zhou, Y. Li, D.Y. Lei, X. Luo, C.W. Qiu, Illusion thermotics, Adv. Mater. 30 (2018) 1707237.
[9] Y. Li, X. Bai, T. Yang, H. Luo, C.W. Qiu, Structured thermal surface for radiative camouflage, Nat. Commun. 9 (2018) 273.
[10] Y. Li, X. Shen, Z. Wu, J. Huang, Y. Chen, Y. Ni, J. Huang, Temperature-dependent transformation thermotics: from switchable thermal cloaks to macroscopic thermal diodes, Phys. Rev. Lett. 115 (2015) 195503.
[11] R. Hu, S. Zhou, X. Yu, X. Luo, Exploring the proper experimental conditions in 2D thermal cloaking demonstration, J. Phys. D 49 (2016) 415302.
[12] H. Xu, X. Shi, F. Gao, H. Sun, B. Zhang, Ultrathin three-dimensional thermal cloak, Phys. Rev. Lett. 112 (2014) 054301.
[13] S. Zhou, R. Hu, X. Luo, Thermal illusion with twinborn-like heat signatures, Int. J. Heat Mass Transf. 127 (2018) 607.
[14] T. Han, X. Bai, J.T. Thong, B. Li, C.W. Qiu, Full control and manipulation of heat signatures: cloaking, camouflage and thermal metamaterials, Adv. Mater. 26 (2014) 1731.
[15] T. Han, J. Zhao, T. Yuan, D.Y. Lei, B. Li, C.-W. Qiu, Theoretical realization of an ultra-efficient thermal-energy harvesting cell made of natural materials, Energy Environ. Sci. 6 (2013) 3537.
[16] R. Hu, X. Wei, J. Hu, X. Luo, Local heating realization by reverse thermal cloak, Sci. Rep. 4 (2014) 3600.
[17] R. Hu, B. Xie, J. Hu, Q. Chen, X. Luo, Carpet thermal cloak realization based on the refraction law of heat flux, EPL 111 (2015) 54003.
[18] Y. Liu, Y. Cheng, R. Hu, X. Luo, Nanoscale thermal cloaking by in-situ annealing silicon membrane, Phys. Lett. A 383 (2019) 2296.
[19] Y. Liu, J. Song, W. Zhao, X. Ren, Q. Cheng, X. Luo, N.X. Fang, R. Hu, Dynamic thermal camouflage via a liquid-crystal-based radiative metasurface, Nanophotonics 9 (2020) 855.

[20] W. Sha, Y. Zhao, L. Gao, M. Xiao, R. Hu, Illusion thermotics with topology optimization, J. Appl. Phys. 128 (2020) 045106.
[21] J. Song, S. Huang, Y. Ma, Q. Cheng, R. Hu, X. Luo, Radiative metasurface for thermal camouflage, illusion and messaging, Opt. Express 28 (2020) 875.
[22] T. Yang, X. Bai, D. Gao, L. Wu, B. Li, J.T. Thong, C.W. Qiu, Invisible sensors: simultaneous sensing and camouflaging in multiphysical fields, Adv. Mater. 27 (2015) 7752.
[23] Y. Ma, Y. Liu, M. Raza, Y. Wang, S. He, Experimental demonstration of a multiphysics cloak: manipulating heat flux and electric current simultaneously, Phys. Rev. Lett. 113 (2014) 205501.
[24] G. Xu, H. Zhang, Y. Jin, S. Li, Y. Li, Control and design heat flux bending in thermal devices with transformation optics, Opt. Express 25 (2017) A419.
[25] G. Xu, H. Zhang, Q. Zou, Y. Jin, Predicting and analyzing interaction of the thermal cloaking performance through response surface method, Int. J. Heat Mass Transf. 109 (2017) 746.
[26] S. Narayana, Y. Sato, Heat flux manipulation with engineered thermal materials, Phys. Rev. Lett. 108 (2012) 214303.
[27] R. Schittny, M. Kadic, S. Guenneau, M. Wegener, Experiments on transformation thermodynamics: molding the flow of heat, Phys. Rev. Lett. 110 (2013) 195901.
[28] F. Yang, B. Tian, L. Xu, J. Huang, Experimental demonstration of thermal chameleonlike rotators with transformation-invariant metamaterials, Phys. Rev. Appl. 14 (2020) 054024.
[29] R. Hu, S. Zhou, W. Shu, B. Xie, Y. Ma, X. Luo, Directional heat transport through thermal reflection meta-device, AIP Adv. 6 (2016) 125111.
[30] I. Peralta, V.D. Fachinotti, J.C. Álvarez Hostos, A brief review on thermal metamaterials for cloaking and heat flux manipulation, Adv. Eng. Mater. 22 (2019) 1901034.
[31] J. Li, Y. Li, T. Li, W. Wang, L. Li, C.-.W. Qiu, Doublet Thermal Metadevice, Phys. Rev. Appl. 11 (2019) 044021.
[32] T. Han, P. Yang, Y. Li, D. Lei, B. Li, K. Hippalgaonkar, C.W. Qiu, Full-parameter omnidirectional thermal metadevices of anisotropic geometry, Adv. Mater. 30 (2018) e1804019.
[33] M. Moccia, G. Castaldi, S. Savo, Y. Sato, V. Galdi, Independent manipulation of heat and electrical current via bifunctional metamaterials, Phys. Rev. X 4 (2014) 021025.
[34] J. Li, Y. Li, P.C. Cao, T. Yang, X.F. Zhu, W. Wang, C.W. Qiu, A continuously tunable solid-like convective thermal metadevice on the reciprocal line, Adv. Mater. 32 (2020) e2003823.
[35] J. Li, Y. Li, W. Wang, L. Li, C.W. Qiu, Effective medium theory for thermal scattering off rotating structures, Opt. Express 28 (2020) 25894.
[36] Y. Li, Y.-.G. Peng, L. Han, M.-.A. Miri, W. Li, M. Xiao, X.-.F. Zhu, J. Zhao, A. Alù, S.J.S. Fan, Anti–parity-time symmetry in diffusive systems, Science 364 (2019) 170.
[37] Y. Li, K.J. Zhu, Y.G. Peng, W. Li, T. Yang, H.X. Xu, H. Chen, X.F. Zhu, S. Fan, C.W. Qiu, Thermal meta-device in analogue of zero-index photonics, Nat. Mater. 18 (2019) 48.
[38] G. Xu, K. Dong, Y. Li, H. Li, K. Liu, L. Li, J. Wu, C.W. Qiu, Tunable analog thermal material, Nat. Commun. 11 (2020) 6028.
[39] L. Xu, J. Wang, G. Dai, S. Yang, F. Yang, G. Wang, J. Huang, Geometric phase, effective conductivity enhancement, and invisibility cloak in thermal convection-conduction, Int. J. Heat Mass Transf. 165 (2021) 120659.
[40] H. Jing, H. Lü, S.K. Özdemir, T. Carmon, F. Nori, Nanoparticle sensing with a spinning resonator, Optica 5 (2018) 1424.
[41] B. Li, R. Huang, X. Xu, A. Miranowicz, H. Jing, Nonreciprocal unconventional photon blockade in a spinning optomechanical system, Photonics Research 7 (2019) 360.
[42] L. Xu, J. Huang, Controlling thermal waves with transformation complex thermotics, Int. J. Heat Mass Transf. 159 (2020) 120133.
[43] L. Zhou, S. Huang, M. Wang, R. Hu, X. Luo, While rotating while cloaking, Phys. Lett. A 383 (2019) 759.